

Research Articles: Behavioral/Cognitive

Attention and capacity limits in perception: A cellular metabolism account

<https://doi.org/10.1523/JNEUROSCI.2368-19.2020>

Cite as: J. Neurosci 2020; 10.1523/JNEUROSCI.2368-19.2020

Received: 3 October 2019

Revised: 10 June 2020

Accepted: 18 June 2020

This Early Release article has been peer-reviewed and accepted, but has not been through the composition and copyediting processes. The final version may differ slightly in style or formatting and will contain links to any extended data.

Alerts: Sign up at www.jneurosci.org/alerts to receive customized email alerts when the fully formatted version of this article is published.

Copyright © 2020 Bruckmaier et al.

This is an open-access article distributed under the terms of the Creative Commons Attribution 4.0 International license, which permits unrestricted use, distribution and reproduction in any medium provided that the original work is properly attributed.

1 **Attention and capacity limits in perception: A cellular metabolism**
2 **account**

3

4 **Abbreviated title:**

5 Attention, perception, and cellular metabolism

6

7 **Authors:**

8 Merit Bruckmaier*¹, Ilias Tachtsidis², Phong Phan², Nilli Lavie¹

9 *corresponding author (Email: merit.bruckmaier.16@ucl.ac.uk)

10

11 **Affiliations:**

12 ¹Institute of Cognitive Neuroscience, University College London, London, UK

13 ²Department of Medical Physics and Biomedical Engineering, University College London,
14 London, UK

15

16 **Conflicts of interest:**

17 The authors declare no conflict of interest.

18

19 **Acknowledgements:**

20 This research was supported by the Economic and Social Research Council and Toyota
21 Motor Europe [grant number ES/J500185/1]. Authors I.T. and P.P. were supported by the
22 Wellcome Trust [grant number 104580/Z/14/Z]. We would also like to thank Paola Pinti for
23 her technical support.

24

25

26

27 Number of pages: 45

28 Number of figures: 4

29 Number of tables: 4

30 Number of words: 250 (abstract), 650 (introduction), 1499 (discussion)

31 **Abstract**

32 Limits on perceptual capacity result in various phenomena of inattentional blindness. Here
33 we propose a neurophysiological account attributing these perceptual capacity limits
34 directly to limits on cerebral cellular metabolism. We hypothesized that overall cerebral
35 energy supply remains constant, irrespective of mental task demand, and therefore an
36 attention mechanism is required to regulate cellular metabolism levels in line with task
37 demands. Increased perceptual load in a task (imposing a greater demand on neural
38 computations) should thus result in increased metabolism underlying attended processing,
39 and reduced metabolism mediating unattended processing. We tested this prediction
40 measuring oxidation states of cytochrome c oxidase (oxCCO), an intracellular marker of
41 cellular metabolism. Broadband near-infrared spectroscopy was used to record oxCCO levels
42 from human visual cortex while participants (both sexes) performed a rapid sequential
43 visual search task under either high perceptual load (complex feature-conjunction search) or
44 low load (feature pop-out search). A task-irrelevant, peripheral checkerboard was presented
45 on a random half of trials. Our findings showed that oxCCO levels in visual cortex regions
46 responsive to the attended-task stimuli were increased in high versus low perceptual load,
47 while oxCCO levels related to unattended processing were significantly reduced. A negative
48 temporal correlation of these load effects further supported our metabolism trade-off
49 account. These results demonstrate an attentional compensation mechanism that regulates
50 cellular metabolism levels according to processing demands. Moreover, they provide novel
51 evidence for the widely-held stipulation that overall cerebral metabolism levels remain
52 constant irrespective of mental task demand and establish a neurophysiological account for
53 capacity limits in perception.

54 **Significance Statement**

55 We investigated whether capacity limits in perception can be explained by the effects of
56 attention on the allocation of limited cellular metabolic energy for perceptual processing.
57 We measured the oxidation state of cytochrome c oxidase, an intracellular measure of
58 metabolism, in human visual cortex during task performance. The results showed increased
59 levels of cellular metabolism associated with attended processing and reduced levels of
60 metabolism underlying unattended processing when the task was more demanding. A
61 temporal correlation between these effects supported an attention-directed metabolism
62 trade-off. These findings support an account for inattention blindness grounded in cellular
63 biochemistry. They also provide novel evidence for the claim that cerebral processing is
64 limited by a constant energy supply, which thus requires attentional regulation.

65

66

67

68

69

70

71

72

73

74 Much research has demonstrated the limited nature of perceptual capacity, reporting that
75 in attention demanding tasks observers can fail to perceive unattended objects, a
76 phenomenon termed “inattention blindness” (e.g. Simons and Chabris, 1999; Cartwright-
77 Finch and Lavie, 2007). Neuroimaging research has attributed inattention blindness to
78 attentional modulations of visual cortex response to unattended stimuli (e.g. Rees, 1999).

79 The level of perceptual load in the task has been shown to be a critical factor in attentional
80 modulations: In tasks involving high perceptual load (e.g. requiring discrimination of feature
81 conjunctions) cortical response to unattended stimuli was found to be smaller compared to
82 low load tasks (e.g. feature detection). For example, high (vs. low) perceptual load in an
83 attended task was shown to result in decreased Blood Oxygen Level Dependent (BOLD)
84 signal in V5/MT in response to unattended motion (Rees et al., 1997), in the
85 parahippocampal cortex in response to task-irrelevant images of ‘places’ (Yi et al., 2004), in
86 V1-V4 in response to flickering checkerboard distractors (Schwartz et al., 2005; Torralbo et
87 al., 2016), and in V4 and TEO in response to unattended, meaningful objects (e.g. flowers,
88 Pinsk et al., 2004). This pattern of findings was obtained across a variety of perceptual load
89 manipulations, all known to increase the computational demand on perceptual capacity
90 (Lavie, 2005; Whiteley and Sahani, 2012; Lavie et al., 2014). Behavioural reports also
91 demonstrated the analogous impact of perceptual load on conscious experience (e.g.
92 Carmel et al., 2007; Macdonald and Lavie, 2008; Stolte et al., 2014).

93 The abundance of studies reporting attentional modulations of the neural response to a
94 variety of stimuli in different cortical regions and across different manipulations of load
95 suggests that they reflect an attentional mechanism which is required to regulate a
96 fundamental, physiological limitation on the overall amount of neural processing. Numerous

97 cellular physiology studies calculating the energy usage of neurons through their ATP
98 consumption have demonstrated that the bio-energetic cost of neural activity is high
99 (Attwell and Laughlin, 2001; Lennie, 2003), primarily because the ion gradients across the
100 cell membrane need to be restored following postsynaptic currents and action potentials.
101 This critically depends on the levels of cellular oxidative metabolism which supplies the
102 required energy in the form of ATP. Other research has shown that the metabolic energy
103 supply to the brain remains constant irrespective of increased mental task demands (Clarke
104 and Sokoloff, 1999). This has led to a widely held premise that cerebral energy supply places
105 a hard limit on mental processing. It follows that increased neural activity (with increased
106 mental-task demand) needs to be balanced out by reductions in cellular metabolism
107 elsewhere. However, while well engrained within theoretical neuroscience, empirical
108 research relating cellular energy limits to limits on mental processing has been rather
109 sparse.

110 Here we investigated this further, directly testing the impact of perceptual processing
111 demands (load) on the attentional allocation of limited cellular metabolism. We
112 hypothesised that cellular metabolism levels are flexibly redistributed between attended
113 and unattended stimuli to compensate for changes in demand on the limited metabolic
114 energy available for neural responses. This ensures that metabolic energy is allocated to
115 goal-relevant processing when the overall neural computational demand exceeds the
116 supply, as in conditions of high perceptual load.

117 In order to provide a straightforward test of this attentional compensatory mechanism that
118 redistributes cellular metabolism according to task demand, a direct assessment of the
119 effect of attention on the underlying cellular metabolism that supplies the required neural

120 energy is necessary. Thus, here we sought to investigate the effects of attention on the
121 distribution of limited cellular metabolic energy to attended versus unattended processing
122 in visual cortex, as assessed with an intra-cellular marker of metabolism levels. We used
123 Broadband Near-Infrared Spectroscopy (BNIRS) which allows us to track the oxidation state
124 of cytochrome c oxidase (oxCCO), a mitochondrial enzyme indicative of cellular oxidative
125 metabolism (Bale et al., 2016 for review), during performance of a selective attention task
126 under different levels of perceptual load.

127

128 **Materials and Methods**

129 ***BNIRS methodology***

130 The oxCCO signal measured with BNIRS provides an intracellular marker of oxidative
131 metabolism levels. Increases in energy requirements due to neuronal activation are largely
132 covered by an upregulation of oxidative phosphorylation whereby energy in the form of ~30
133 adenosine triphosphate molecules (ATP, commonly known as the molecular unit of currency
134 for intracellular transfer of energy) per glucose molecule are produced (Attwell et al., 2010;
135 Lin et al., 2010). CCO is the final electron acceptor of the electron transport chain in the
136 mitochondria where oxidative phosphorylation takes place. Since its concentration does not
137 change over relatively short time periods (e.g. hours), the ratio between oxidised and
138 reduced CCO can be used to assess changes to the level of cellular metabolism. BNIRS can
139 measure the oxCCO signal by using the full light spectrum in the range of 780-900nm (Arifler
140 et al., 2015). Conventional fNIRS systems, in contrast, have just 2-3 wavelengths of light and
141 thus can only be used to measure concentration changes in oxygenated (HbO₂) and

142 deoxygenated (HHb) haemoglobin in the blood vessels surrounding the brain areas of
143 interest. The intracellular BNIRS measure of oxCCO has been validated both in animal and
144 human studies, for example demonstrating its correlation with phosphorous magnetic
145 resonance spectroscopy (^{31}P MRS) measures of nucleotide triphosphate levels (NTP, which is
146 mainly ATP; Peeters-Scholte et al., 2004; Bainbridge et al., 2014; Kaynezhad et al., 2019) and
147 measures of the lactate/pyruvate ratio, a marker of aerobic metabolism (i.e. mitochondrial
148 ATP synthesis), as obtained with micro dialysis (Tisdall et al., 2008). For a review see Bale et
149 al. (2016).

150 In the present study, we used a multi-channel BNIRS system, which has been developed to
151 specifically measure oxCCO (e.g. Phan et al., 2016) and has been shown to successfully
152 isolate its signal (based on the absorption characteristics of oxCCO, which has a broad peak
153 at 830nm) from other chromophores (HHb and HbO₂), as described here (Siddiqui et al.,
154 2018). The instrument has four source and ten detector fibres (optodes) and a sampling rate
155 of 1 s. The detectors were arranged in rows of five with the four sources between them
156 (source detector separation was 30mm), resulting in 16 measurement channels. The array
157 was fitted horizontally in a custom-designed optode holder, the centre of which was placed
158 4cm above theinion. All optode positions were digitised using a Patriot Digitizer (Polhemus,
159 Colchester, Vermont, USA), and theinion, nasion, left and right preauricular points, O1, O2,
160 and vertex served as reference points (based on 10/20 electrode placement system). To
161 ensure that the positions of the channels matched between participants the digitized
162 locations were converted to MNI coordinates using NIRS SPM (Ye et al., 2009).

163

164

165 ***Experiment 1: Experimental Design and Statistical Analysis***

166 In Experiment 1 we first sought to establish whether the metabolism levels associated with
167 unattended processing are affected by the level of perceptual load in the attended task. To
168 that purpose we have used a well-established perceptual load manipulation which includes
169 a rapid, serial visual search task that is accompanied by a task-irrelevant, flickering
170 checkerboard in the periphery on half of the trials (Schwartz et al., 2005; Carmel et al., 2011;
171 Ohta et al., 2012). We examined the effects of perceptual load in the attended task on the
172 levels of metabolism specifically associated with the unattended, peripheral checkerboard.
173 Since the purpose of Experiment 1 was to investigate whether perceptual load can
174 modulate the levels of metabolism associated with the processing of unattended stimuli,
175 the size of the checkerboard was maximised (relative to the attended task stimuli) to ensure
176 that we would be able to measure a strong signal associated with unattended stimulus
177 processing in the low load condition, as well as a modulation of this response under high
178 perceptual load.

179 Participants

180 16 participants (11 female, age range 18-34) took part in Experiment 1. Since this is the first
181 study using fNIRS to measure effects of attention on visual processing, no formal sample
182 size calculations could be carried out. We therefore used a sample size that is comparable to
183 studies using other neuroimaging techniques, looking at similar effects of perceptual load on
184 cortical processing (e.g. Schwartz et al., 2005, 16 participants; Molloy et al., 2015, 14
185 participants; Torralbo et al., 2016, 18 participants). A sensitivity analysis on the results
186 obtained in this experiment, using MorePower (Campbell and Thompson, 2012), confirmed
187 that this sample size was sufficient to detect effects of a size $\eta_p^2 \geq 0.37$ with a power of

188 80%. All participants had normal or corrected to normal vision and normal colour vision.
189 This research was approved by the UCL research ethics committee, and written, informed
190 consent was obtained from all participants prior to data collection.

191 Task and Stimuli

192 The experiment took place in a darkened room to minimise external light interfering with
193 the BNIRS system. We presented the experiments with Matlab Cogent Graphics tool box.
194 The attended task display consisted of a series of crosses (each $0.08^\circ \times 0.06^\circ$ of visual angle),
195 coloured either blue (0 115 255), green (0 255 0), yellow (255 255 0), purple (160 32 240),
196 red (255 0 0), or brown (156 102 31), and oriented either upright or inverted. These stimuli
197 were presented rapidly in the centre of the computer screen on a black background (see
198 Figure 1, and see Schwartz et al., 2005 and Carmel et al., 2011). On half of the streams a
199 black and white, radial checkerboard, which was flickering at a frequency of 7 Hz, was
200 present in the periphery of the visual field (extending 17° of visual angle from the centre of
201 the screen, leaving out a circle with a radius of 0.7° in the centre where the targets were
202 presented). Participants were instructed to ignore the checkerboard stimulus, if present.
203 Their task was to detect pre-specified 'target' crosses by pressing the '0' key on the number
204 pad of the computer keyboard. In the low load condition the targets were determined by
205 colour alone (any red crosses), whereas in the high load condition targets were determined
206 by a conjunction of colour and orientation (upright purple and inverted blue crosses).

207 Each 32 item stream started with a fixation cross present for 1000 ms at the centre of the
208 screen, followed by the presentation of 32 crosses (250 ms), each followed by a 500 ms ISI.
209 Each stream contained 4 targets (12.5% of stimuli) that were presented randomly in any
210 temporal stream positions except for the first, with the constraint that no two targets could

211 appear on successive presentations. The time window of 750 ms from the onset of a target
212 has previously been shown to provide sufficient time for typical responses to be made
213 before the next stimulus appeared (e.g. Carmel et al., 2011). However, the constraint that
214 no two targets could appear in succession allowed us to accept any target detection
215 response made within the 1500 ms time window from target onset (the minimal time
216 between two potential targets) as correct. The target stimulus was equally likely to be in
217 either orientation in the low load or colour/orientation combination in the high load
218 condition (sampled randomly with replacement). Apart from excluding the target colour (in
219 the low load) and target colour/orientation combination (in the high load), all colours and
220 colour/orientation combinations were equiprobable for each of the non-target stimuli
221 (sampled randomly with replacement), with the exception that the opposite feature
222 combination of those defining the targets in the high load condition (i.e. upright blue and
223 inverted purple) were twice as likely as any other non-target colour/orientation
224 combination. To match the streams across the load conditions, these opposite combinations
225 were also twice as likely in the low load streams. Note, that the visual stimulation was thus
226 the same in both load conditions and load was varied just through the task instructions
227 which required a different amount of perceptual processing for the same stimulus stream.
228 Participants completed 56 streams, each consisting of 32 items, lasting for 25 s, and
229 followed by a 25 s break, during which participants received automated feedback on their
230 performance. Five seconds before the next stream, instructions indicating the new targets
231 appeared on the screen. Participants started with two short practice streams (one per load
232 condition, always starting with low load). The experimental streams were interleaved in an
233 ABBABAAB pattern with respect to the load condition.

234 Data Pre-processing

235 In order to convert the measured attenuation changes across the wavelengths between
236 780-900nm into concentration changes of the chromophores (deoxygenated haemoglobin
237 (HHb), oxygenated haemoglobin (HbO₂), oxCCO), we applied the UCLn algorithm using the
238 Modified Beer-Lambert law assuming a differential pathlength factor (DPF) of 6.26 and its
239 wavelength dependence (Phan et al., 2016). Next, the concentration changes of each
240 chromophore were bandpass filtered to remove physiological noise (such as Mayer waves)
241 using a 5th order Butterworth filter with cut-off frequencies of 0.01 and 0.08 Hz. Streams
242 were excluded from analysis if motion artefacts were present, or if the error rate was
243 particularly high ($\geq 75\%$), potentially indicating that the participant was responding to the
244 wrong targets. This resulted in 3.46% of trials in total removed in Experiment 1 and 6.05% of
245 trials removed in Experiment 2. For each participant and channel, the data was then
246 prepared by averaging across the RSVP streams for each of the four conditions (high/low
247 load x checkerboard present/absent), using the first second of each RSVP stream as the
248 baseline by subtracting it from the activity in the rest of the trial.

249 The converted MNI coordinates indicated that our channel positions were located across
250 Brodmann areas 17, 18, and 19 – commonly referred to as striate cortex and visual
251 association areas. Based on their MNI coordinates, measurement channels were allocated
252 individually for each participant (Ye et al., 2009) to the following cortical regions: left and
253 right BA19, left and right BA18, and BA17 (see Table 1 and 2 for average coordinates and
254 allocation of each channel in Experiment 1 and 2, respectively). This step reduced the
255 number of statistical comparisons compared to the channel level, and therefore lowered the
256 risk of false positives.

257 Statistical Analysis

258 In both Experiments 1-2 analyses of the oxCCO were based on the mean oxCCO signal in
259 each of the conditions for each participant across the 25s task period. In all analyses of both
260 the oxCCO and the behavioural data the outlier exclusion criterion was based on responses
261 that are > 2.5 SD from the group mean. This resulted in the exclusion of one participant in
262 each of the experiments. Behavioural responses were compared using pairwise, two-tailed t
263 tests comparing response times, hit rates, and false alarm rates between high vs. low load
264 conditions. The main oxCCO analysis used a 2 x 2 within-subject ANOVA to investigate the
265 effects of distractor presence (present vs. absent) and perceptual load (high vs. low).
266 Statistical significance is reported using an alpha level of .05 with false discovery rate (FDR)
267 correction (Benjamini and Hochberg, 1995) for multiple comparisons across the five cortical
268 regions.

269 ***Experiment 2: Experimental Design and Statistical Analysis***

270 In Experiment 2, we investigated whether the modulation of the metabolism associated
271 with unattended processing in Experiment 1 was the result of a load-induced trade-off, as
272 suggested by previous functional imaging experiments (Pinsk et al., 2004; Torralbo et al.,
273 2016). We therefore examined whether the reduction of metabolic energy associated with
274 unattended processing by high perceptual load was accompanied by a simultaneous
275 increase in metabolism underlying attended processing. To that purpose we have modified
276 the task used to increase its sensitivity to reveal the effects of load on the attended stimuli,
277 as follows: The size of the central crosses was substantially increased in order to produce a
278 greater oxCCO signal. Furthermore, a white pattern of swirls was overlaid over each cross to

279 increase the changes in local contrast and therefore to further increase the extent to which
280 the attended stimuli activated striate and extrastriate visual cortex regions (see Figure 1).

281 Participants

282 Power analysis using MorePower (Campbell and Thompson, 2012) based on the effect sizes
283 observed in Experiment 1 indicated that a sample of 12-18 participants (depending on which
284 Brodmann Area was used for the calculation) is required to detect the load effect on
285 unattended processing with $\alpha = .05$ and 80% power. We collected data from 18 participants
286 (15 female, age range 20-38), which satisfies the more conservative estimate of sample size,
287 all with normal or corrected to normal vision and normal colour vision. One participant
288 participated in both experiments, the rest were naïve.

289 Task and Stimuli

290 In order to establish load effects on metabolism associated with attended processing (in
291 addition to unattended processing), we increased the size of the central crosses (vertical
292 bar: height: 23.7°, width: 5.1°; horizontal bar: height: 2.1°, width: 6.7°; midline of horizontal
293 bar was placed at 6.1° from the (top/bottom) end of the vertical bar) and overlaid them with
294 a white pattern of swirls to increase the local contrast and therefore the extent to which
295 they activate early visual cortex regions (see Figure 1). The distractors were two flickering,
296 radial checkerboard segments on either side of the central task (147° of arc, with a radius
297 extending 12.8° of visual angle from the centre of the screen, leaving a circle of 5.7° in
298 radius free in the centre). Thus, both the attended and unattended stimuli should now elicit
299 a measurable signal that allows us to track any modulation induced by changes to
300 perceptual load. Since the stimuli were far larger now, we ensured that participants would

301 still fixate at the centre of the stimuli in order to process both the bottom and the top
302 horizontal cross bars, and avoid a strategy of judging the horizontal bar location not just by
303 its presence but also from its absence at one fixated position (either the top or the bottom
304 of each cross), by including non-target stimuli that consisted only of the vertical bar of the
305 cross on a random third of stimulus presentations (colours selected in random from the
306 stimulus set irrespective of whether non-target or target colours). Subjects were instructed
307 to withhold responses to these stimuli (including when presented in the target colour in the
308 low load conditions). All other details remained the same as in Experiment 1.

309 Statistical Analysis

310 Following the same exclusion criteria as for Experiment 1, one subject was excluded from
311 analysis in Experiment 2. Areas showing significant effects in Experiment 1 served as regions
312 of interest (ROI; bilaterally) for the within-subject 2 x 2 (load by distractor conditions)
313 ANOVAs in Experiment 2, while FDR correction was applied to all other analyses (including
314 the attended processing analysis) since the regions for these have not been previously
315 established. For this reason, the simple main effects concerning attended processing
316 (distractor absent conditions) were not reported in the ROI-based 2 x 2 ANOVAs (of
317 distractor condition by load). In addition to the same ANOVAs as those run in Experiment 1,
318 we also performed pairwise t-tests to compare the mean oxCCO response during the 25 s
319 task period in distractor absent trials in high versus low perceptual load, which reflects the
320 activity associated specifically with the processing of the attended task stimuli (without
321 distractor stimuli).

322 In Experiment 2, we also analysed the temporal correlation of the load effect on attended
323 processing (High Absent – Low Absent) and unattended processing ((High Present – High

324 Absent) – (Low Present – Low Absent)), during the 25 s task period. The group mean for
325 each second-by-second time point in each time series was computed, following a trial
326 splitting procedure that was conducted to ensure the data entered into each participant’s
327 time series did not include overlapping trials (since the distractor absent condition was used
328 for both the attended and unattended signal), as follows. We split the distractor absent raw
329 data randomly into two halves for each participant: One half was used for the attended time
330 series and the other used for the unattended time series, before the two time series got
331 averaged across all participants to provide the group mean for each second-by-second data
332 point in the two time series. A Kolmogorov-Smirnov test verified that the data was normally
333 distributed and therefore suitable for a Pearson correlation. To avoid sample bias from the
334 random splitting of the data we repeated the random data split 1000 times and a Pearson
335 correlation was conducted on the attended vs. unattended time series in each of the 1000
336 samples. We note that this correlation analysis treats subjects as fixed rather than random
337 effects, and thus only allows inferences about the specific sample, not the whole
338 population. A replication of this analysis with a larger sample (that allows for a correlation
339 analysis that treats subjects as random effects) is important to further support the temporal
340 “push and pull” nature of the resource trade-off we have observed.

341 In order to assess significance of the mean r we used a permutation test with 10,000
342 permutations, using the same 1000 samples but with randomly assigned condition labels (to
343 each participant’s time series in each sample). A significance threshold of 95% was then
344 used for the comparison of the mean r value obtained from the correctly labelled data with
345 the distribution of 10,000 mean r values from the random permutations (i.e. to be
346 considered significant the mean r value from the correctly labelled data had to be greater

347 than 9500 of the mean r values obtained from the data with randomly shuffled condition
348 labels). The use of the permutation analysis controls for any effects of dependence of data
349 points within each subject in the correlated time-series (e.g. autocorrelation), since these
350 are equally present in the time-series with permuted condition labels.

351

352 **Results**

353 ***Experiment 1***

354 Behavioural Data

355 Behavioural results (see Table 3) confirmed that higher perceptual load in the attended task
356 increased task reaction times ($t(14) = 18.36, p < 0.001, d = 5.19$), reduced hit rates ($t(14) = -$
357 $3.41, p = 0.004, d = -0.90$), and increased the number of false alarms ($t(14) = 3.76, p = 0.002,$
358 $d = 1.06$), thus confirming the efficacy of the perceptual load manipulation.

359 oxCCO Data

360 The oxCCO results are shown in Figure 2. As can be seen in panel 2A, the mean oxCCO
361 response during the task period was larger when the distractor was present than when it
362 was absent, as was confirmed with a main effect of distractor presence in all BAs (left BA19:
363 $F(1,14) = 12.53, p_{FDR} = 0.005, \eta_p^2 = 0.47$; left BA18: $F(1,14) = 24.61, p_{FDR} < 0.001, \eta_p^2 = 0.65$;
364 BA17: $F(1,14) = 27.85, p_{FDR} < 0.001, \eta_p^2 = 0.67$; right BA18: $F(1,14) = 6.28, p_{FDR} = 0.031, \eta_p^2 =$
365 0.31 ; right BA19: $F(1,14) = 4.81, p_{FDR} = 0.046, \eta_p^2 = 0.26$. Importantly, Figure 2 (B-C) also
366 shows that the oxCCO signal associated with the distractor presence (vs. absence) was
367 reduced in the high (compared to low) load conditions, as predicted. This interaction effect

368 (of load and distractor conditions) was significant in BA17 ($F(1,14) = 9.10$, $p_{FDR} = 0.023$, $\eta_p^2 =$
369 0.39), right BA18 ($F(1,14) = 6.84$, $p_{FDR} = 0.034$, $\eta_p^2 = 0.32$), and right BA19 ($F(1,14) = 12.25$,
370 $p_{FDR} = 0.018$, $\eta_p^2 = 0.47$). Indeed, in both right BA18 and right BA19 the distractor effect was
371 only significant in the low load conditions (right BA18: $t(14) = 3.18$, $p = 0.007$; right BA19:
372 $t(14) = 3.26$, $p = 0.006$), but not in the high load conditions (right BA18: $t(14) = 1.18$, $p =$
373 0.259 ; right BA19: $t(14) = 0.39$, $p = 0.704$), while in BA 17 it remained significant in both load
374 conditions (low load: $t(14) = 5.87$, $p < 0.001$; high load: $t(14) = 3.69$, $p = 0.002$). Similar
375 trends of the load-distractor interaction did not reach significance in left BA18 ($F(1,14) =$
376 3.39 , $p_{FDR} = 0.110$) and left BA19 ($F(1,14) = 2.25$, $p_{FDR} = 0.156$). There was no main effect of
377 perceptual load in any area (all $p_{FDR} > 0.813$), as might be expected given the terminative
378 nature of the interaction. Finally, a comparison of the baselines used in the low load and
379 high load revealed no significant difference (mean difference $\leq 0.0042 \mu\text{M}$, all $p_{FDR} > 0.655$).

380

381 **Experiment 2**

382 In order to further establish whether the observed reduction of the oxCCO signal related to
383 unattended processing in Experiment 1 results from a resource trade-off relationship with
384 the attended processing, in Experiment 2 we compared the impact of perceptual load on
385 cellular metabolism levels in attended versus unattended processing using modified task
386 stimuli better suited to reveal BNIRS signals from both types of stimuli.

387 Behavioural Data.

388 As in Experiment 1, behavioural results (see Table 4) showed that high perceptual load
389 increased reaction times ($t(16) = 16.08$, $p < 0.001$, $d = 3.90$), reduced hit rates ($t(16) = -2.83$,

390 $p = 0.012$, $d = -0.69$), and increased false alarm rates ($t(16) = 2.17$, $p = 0.046$, $d = 0.53$), thus
391 successfully manipulating task demand.

392 oxCCO Data

393 The oxCCO results of Experiment 2 are shown in Figure 3. As can be seen in the figure, the
394 effect of perceptual load on distractor processing found in Experiment 1 was replicated in
395 Experiment 2. Specifically, Figure 3A shows that the mean oxCCO response during the task
396 period was larger when the distractor was present as compared to when it was absent, and
397 this was reflected in the significant main effects of distractor presence (vs. absence) in left
398 BA18 ($F(1,16) = 6.68$, $p = 0.012$, $\eta_p^2 = 0.29$), right BA18 ($F(1,16) = 5.24$, $p = 0.036$, $\eta_p^2 = 0.25$)
399 and right BA19 ($F(1,16) = 6.10$, $p = 0.025$, $\eta_p^2 = 0.28$). Similar trends did not reach
400 significance in left BA19 ($F(1,16) = 3.77$, $p = 0.070$) and BA17 ($F(1,16) = 2.84$, $p = 0.111$).
401 Importantly, Figure 3B and D show that, as in Experiment 1, the oxCCO signal change
402 associated with the presence (vs. absence) of the distractor was reduced in the high (vs.
403 low) perceptual load conditions and this was confirmed by significant interactions between
404 load and distractor presence in left BA18 ($F(1,16) = 7.51$, $p = 0.015$, $\eta_p^2 = 0.32$) and right
405 BA19 ($F(1,16) = 4.74$, $p = 0.045$, $\eta_p^2 = 0.23$). In both areas the distractor presence (vs.
406 absence) effect was significant in the low load (left BA18: $t(16) = 4.07$, $p = 0.001$; right BA19:
407 $t(16) = 3.54$, $p = 0.003$) but not the high load conditions (left BA18: $t(16) = 0.53$, $p = 0.600$;
408 right BA19: $t(16) = 0.47$, $p = 0.648$). Similar interaction trends did not reach significance in
409 the other BAs (all $F < 3.22$, $p > 0.092$). There were no main effects of load in any areas apart
410 from BA17 which showed a significantly increased signal in the high load compared to the
411 low load conditions ($F(1,16) = 4.91$, $p = 0.041$, $\eta_p^2 = 0.23$; $F < 1.23$, $p > 0.28$ in all other

412 areas). Finally, as in Experiment 1, no significant difference was found between the
413 baselines of high and low load conditions (mean difference $\leq 0.0032 \mu\text{M}$; all $p_{\text{FDR}} > 0.131$).

414 To assess the impact of perceptual load on attended processing, we analysed the effect of
415 load on the oxCCO signal related to the attended stream in the distractor-absent (target
416 only) conditions in all areas. As can be seen in Figure 3A and C, the mean oxCCO response to
417 the targets (in the distractor absent conditions) was increased under high perceptual load,
418 and this reached significance in left BA18 ($t(16) = 2.98$, $p_{\text{FDR}} = 0.022$, $d = 0.72$) and BA17
419 ($t(16) = 3.49$, $p_{\text{FDR}} < 0.015$, $d = 0.85$). Similar trends in the other BAs failed to reach
420 significance (all $t < 1.63$, $p_{\text{FDR}} > 0.169$).

421 In addition, we assessed the temporal correlation between the effects of load on oxCCO
422 levels related to attended processing and the load effects on oxCCO levels related to
423 unattended processing during the 25 s task period. The results are shown in Figure 4. As can
424 be seen in the figure, the temporal (second by second) patterns of the effects of load on
425 attended and unattended signals were negatively correlated in all areas. A random
426 permutation test (for details on this analysis see Materials and Methods) showed that all
427 these correlations were significant (left BA19: mean $r = -0.38$, $p_{\text{FDR}} < 0.001$; left BA18: mean r
428 $= -0.43$, $p_{\text{FDR}} < 0.001$; BA17: mean $r = -0.31$, $p_{\text{FDR}} < 0.001$; right BA18: mean $r = -0.12$, $p_{\text{FDR}} <$
429 0.001 ; right BA19: mean $r = -0.43$, $p_{\text{FDR}} < 0.001$). These findings indicate a “push-pull” trade-
430 off relationship between metabolism levels related to attended and unattended processing
431 as a function of perceptual load in the task.

432 Finally, the hypothesis of constant energy supply irrespective of mental task demand (i.e.
433 perceptual load) receives additional support when oxCCO levels are measured while both
434 attended and unattended stimuli are present. As shown in Figure 3A (distractor present

435 conditions) metabolism levels remain constant across the low load and high load conditions
436 in all five regions when thus measured (all $p_{\text{FDR}} > 0.440$). This is explained by a spill-over to
437 the processing of the distractor in the low load conditions but not high load conditions
438 which are likely to approach the set energy limit already with the attended processing
439 alone.

440

441 **Discussion**

442 The present results provide support for our proposed cellular metabolism account for
443 perceptual capacity limits and the role of attention in perception. Specifically, the findings
444 established attention-dependent modulation of cellular metabolism levels in visual cortex in
445 line with the changes in perceptual load levels in the task. Higher perceptual load in the task
446 was associated with increased cellular metabolism levels related to attended processing and
447 reduced levels related to unattended processing in the form of a direct resource trade-off.
448 This “push-pull” relationship is further supported by a negative correlation between the
449 temporal pattern of load effects on metabolism levels associated with attended versus
450 unattended processing. Perceptual capacity limits and the consequent effects of reduced
451 unattended processing in conditions of high perceptual load may therefore be attributed to
452 a shortage in cellular metabolism for processing stimuli outside the focus of attention.

453 Our account offers a neurobiological explanation of the large body of studies showing
454 attentional modulations of task performance and perception as well as the related cortical
455 activity due to high perceptual load in the task. The previous findings have been obtained
456 with a variety of behavioural tasks and attentional manipulations (Simons and Chabris,

457 1999; Carmel et al., 2007; Cartwright-Finch and Lavie, 2007; Macdonald and Lavie, 2008;
458 Murphy and Greene, 2016) and in functional imaging studies (Rees et al., 1997; Handy and
459 Mangun, 2000; Handy et al., 2001; Pinsk et al., 2004; Yi et al., 2004; Schwartz et al., 2005;
460 Nagamatsu et al., 2011; Parks et al., 2013; Molloy et al., 2015; Torralbo et al., 2016). The
461 present results suggest that these well-established modulations can be explained by
462 changes in cellular metabolism levels in visual cortex.

463 Importantly, oxCCO levels provide a direct, intracellular measure of neural metabolism due
464 to the CCO enzyme's integral role in cellular oxygen metabolism (as the final electron
465 acceptor in the respiratory electron transport chain of the mitochondria). In contrast, the
466 haemodynamic response measured with fMRI cannot be used to directly infer the level of
467 underlying cellular metabolism, despite being correlated with it (Logothetis, 2008).
468 Specifically, the level of deoxygenated haemoglobin in local blood vessels, underlying the
469 BOLD response, is not only influenced by the level of cellular oxygen metabolism, but in
470 even greater measure by the rate of cerebral blood flow (CBF; Fox and Raichle, 1986; Buxton
471 and Frank, 1997). While oxygen metabolism is driven by the energy demand following
472 neural activity, increases in CBF are thought to be driven primarily by the presence of the
473 excitatory neurotransmitter glutamate – these two processes can therefore be considered
474 as related, but operating in parallel (Attwell and Iadecola, 2002). Moreover, the ill-
475 understood, variable coupling of the two over space and time further complicates any
476 inference about oxygen metabolism (Logothetis, 2008; Lindquist et al., 2009).

477 The present findings also lend support to the influential (e.g. Raichle and Gusnard, 2002;
478 Lennie, 2003; Carrasco, 2011; Lauritzen et al., 2012) notion that overall cerebral metabolism
479 remains constant irrespective of mental task demand (Sokoloff et al., 1955), and despite the

480 high energetic cost of neural firing (Attwell and Laughlin, 2001; Lennie, 2003). While much
481 theoretical and modelling work presumed this notion, subsequent empirical evidence for
482 this claim has been scarce. In a repeatedly cited study Sokoloff et al. (1955, see also Clarke
483 and Sokoloff, 1999) used a nitrous oxide technique as a measure of whole-brain cerebral
484 metabolic rate (CMRO₂). Overall CMRO₂ during rest did not significantly differ from overall
485 CMRO₂ during a mental (arithmetic) task condition. While often cited as evidence for a
486 constant and therefore limited metabolic energy capacity of the human brain, this
487 conclusion rests on a null result. Here, we similarly report constant oxCCO levels irrespective
488 of mental task demand (i.e. load) when these are measured as summed activity across both
489 attended and unattended processing. This finding was expected based on load theory
490 predictions that spare capacity spills over to the processing of unattended stimuli in low
491 perceptual load conditions, so that the overall level of metabolism remains the same as in
492 high load conditions (when more capacity is exhausted by attended processing). Thus, just
493 the distribution between attended and unattended processing differs between load
494 conditions. Importantly, we additionally report findings that positively demonstrate this
495 trade-off effect of mental processing demand on cerebral metabolism levels related to
496 attended versus unattended processes. This finding, alongside the temporally specific
497 correlation of load effects, directly supports the commonly made assertion that limited
498 metabolic resources are redistributed in order to flexibly adapt to mental task demands
499 (Raichle et al., 2001; Carrasco, 2011), highlighting the role of attention in control over the
500 metabolic resource allocation. We suggest that the observed trade-off is the result of an
501 attention mechanism that serves to balance metabolic supply and demand across the brain,
502 in line with current processing priorities.

503 Our results fit with the well-established findings that increases in cellular metabolism during
504 enhanced neural firing are primarily needed for the energetically expensive process of
505 restoring ion gradients after depolarisation of the cell membrane. The observed pattern of
506 responses therefore reflects changes in the number of action potentials sent within the area
507 of measurement. However, a considerable contribution to the signal is likely also made by a
508 change in the number of incoming signals (i.e. post-synaptic potentials). The integration of
509 post-synaptic potentials has been shown to require more metabolism than firing action
510 potentials (Schwartz et al., 1979), suggesting this may contribute more to our observed
511 effects than just action potential generation. Since attention is known to involve extensive
512 feedback-connections between higher level areas (frontal and parietal cortices) and sensory
513 cortices (Dehaene et al., 1998; Silvanto et al., 2009; Wei et al., 2013; Torralbo et al., 2016),
514 incoming signals from these areas likely play a role in the changes in metabolic patterns
515 observed here in visual cortex, in addition to incoming signals from lower level areas and
516 local connections.

517 It is also important to consider how the present results relate to previous behavioural
518 findings. The perceptual load manipulation used in our study is well established (Schwartz et
519 al., 2005; Bahrami et al., 2007; Carmel et al., 2011; Ohta et al., 2012) and known to converge
520 with other manipulations of perceptual load (e.g. spatial visual search, set-size
521 manipulations) to demonstrate reduced unattended processing, leading to “inattentive
522 blindness”. Importantly, these effects are found with both implicit measures of unattended
523 processing (e.g. neuroimaging, distractor effects on RT) which are collected for concurrent
524 attended and unattended processing, as here, and explicit detection sensitivity measures,
525 including measures of detection responses made immediately upon appearance (e.g.

526 Macdonald and Lavie, 2008; Lavie et al., 2014) which rule out alternative accounts
527 attributing inattention blindness to ‘inattention amnesia’. The convergence of findings
528 suggests alternative accounts of the present findings in terms of task-specific factors are
529 unlikely. For example, while the current task included an extra feature to be remembered in
530 high load (low load: upright or inverted red cross; high load: upright purple or inverted blue
531 cross), and thus perhaps increased visual short term memory (VSTM) load, other feature-
532 versus-conjunction load manipulations that equated the number of features have found
533 consistent results (Wojciulik and Kanwisher, 1999; Stolte et al., 2014). Moreover, VSTM load
534 is known to affect unattended processing in the same way as perceptual load, unlike other
535 types of WM load that tap more into cognitive control ((Lavie et al., 2004; Konstantinou et
536 al., 2012,2014; Konstantinou and Lavie, 2013), and since VSTM has been shown to recruit
537 sensory cortices (e.g. Pasternak and Greenlee, 2005), the explanation of our results based
538 on a metabolic resource trade-off in visual cortex still applies.

539 Finally, our metabolism trade-off account opens up many novel questions for future
540 research regarding the nature of capacity limits – for instance regarding the spatial scale of
541 the trade-off and whether it extends to multimodal processes. Furthermore, while we
542 demonstrated that attention can lead to the flexible redistribution of metabolism based on
543 task demand, this may also occur in spatial cueing or feature-based attention paradigms.
544 Future research should investigate whether such manipulations of attentional engagement
545 lead to similar metabolism trade-offs.

546 **Conclusion**

547 The concept of a mental processing resource with limited capacity has dominated attention
548 research for decades (Navon and Gopher, 1979; Wickens et al., 1984; Lavie et al., 2014;

549 Molloy et al., 2019), however, its relationship to the biochemical resources mediating neural
550 activity remained unclear. Here, we provide evidence for our proposal that this frequently-
551 theorized, capacity-limited, mental resource corresponds to limited cellular metabolic
552 energy across the brain. Our findings demonstrate that the level of perceptual load in the
553 task modulates the impact of attention on cellular metabolism levels in visual cortex regions
554 related to stimulus perception. Increased perceptual load leads to increased levels of
555 metabolism underlying attended processing, at the expense of unattended processing, thus
556 explaining phenomena of inattention blindness. Moreover, this resource trade-off
557 supports the notion that the overall cerebral metabolic energy supply remains constant
558 irrespective of mental task demand, by demonstrating how localised increases in processing
559 demand, and the associated demand for metabolic energy, are balanced out by localised
560 decreases in metabolism elsewhere, to maintain a constant level overall.

561

562

563

564

565

566

567

568

569

570 **References**

- 571 Arifler D, Zhu T, Madaan S, Tachtsidis I (2015) Optimal wavelength combinations for near-
572 infrared spectroscopic monitoring of changes in brain tissue hemoglobin and
573 cytochrome c oxidase concentrations. *Biomed Opt Express* 6:933.
- 574 Attwell D, Buchan AM, Charpak S, Lauritzen M, MacVicar BA, Newman EA (2010) Glial and
575 neuronal control of brain blood flow. *Nature* 468:232–243.
- 576 Attwell D, Iadecola C (2002) The neural basis of functional brain imaging signals. *Trends*
577 *Neurosci* 25:621–625.
- 578 Attwell D, Laughlin SB (2001) An Energy Budget for Signaling in the Grey Matter of the Brain.
579 *J Cereb Blood Flow Metab* 21:1133–1145.
- 580 Bahrami B, Lavie N, Rees G (2007) Attentional Load Modulates Responses of Human Primary
581 Visual Cortex to Invisible Stimuli. *Curr Biol* 17:509–513.
- 582 Bainbridge A, Tachtsidis I, Faulkner SD, Price D, Zhu T, Baer E, Broad KD, Thomas DL, Cady
583 EB, Robertson NJ, Golay X (2014) Brain mitochondrial oxidative metabolism during and
584 after cerebral hypoxia-ischemia studied by simultaneous phosphorus magnetic-
585 resonance and broadband near-infrared spectroscopy. *Neuroimage* 102:173–183.
- 586 Bale G, Elwell CE, Tachtsidis I (2016) From Jöbsis to the present day: a review of clinical near-
587 infrared spectroscopy measurements of cerebral cytochrome-c-oxidase. *J Biomed Opt*
588 21:091307.
- 589 Benjamini Y, Hochberg Y (1995) Controlling the False Discovery Rate: A Practical and
590 Powerful Approach to Multiple Testing. *J R Stat Soc Ser B* 57:289–300.

- 591 Buxton RB, Frank LR (1997) A Model for the Coupling between Cerebral Blood Flow and
592 Oxygen Metabolism during Neural Stimulation. *J Cereb Blood Flow Metab* 17:64–72.
- 593 Campbell JID, Thompson VA (2012) MorePower 6.0 for ANOVA with relational confidence
594 intervals and Bayesian analysis. *Behav Res Methods* 44:1255–1265.
- 595 Carmel D, Saker P, Rees G, Lavie N (2007) Perceptual load modulates conscious flicker
596 perception. *J Vis* 7:14.
- 597 Carmel D, Thorne JD, Rees G, Lavie N (2011) Perceptual load alters visual excitability. *J Exp*
598 *Psychol Hum Percept Perform* 37:1350–1360.
- 599 Carrasco M (2011) Visual attention: The past 25 years. *Vision Res* 51:1484–1525.
- 600 Cartwright-Finch U, Lavie N (2007) The role of perceptual load in inattention blindness.
601 *Cognition* 102:321–340.
- 602 Clarke D, Sokoloff L (1999) Circulation and Energy Metabolism of the Brain. In: *Basic*
603 *Neurochemistry: Molecular, Cellular and Medical Aspects.*, 6th ed. (Siegel G, Agranoff
604 B, Albers R, Fisher S, Uehler M, eds), pp 637–669. Philadelphia: Lippincott-Raven.
- 605 Dehaene S, Kerszberg M, Changeux J-P (1998) A neuronal model of a global workspace in
606 effortful cognitive tasks. *Proc Natl Acad Sci* 95:14529–14534.
- 607 Fox PT, Raichle ME (1986) Focal physiological uncoupling of cerebral blood flow and
608 oxidative metabolism during somatosensory stimulation in human subjects. *Proc Natl*
609 *Acad Sci U S A* 83:1140–1144.
- 610 Handy TC, Mangun GR (2000) Attention and spatial selection: Electrophysiological evidence
611 for modulation by perceptual load. *Percept Psychophys* 62:175–186.

- 612 Handy TC, Soltani M, Mangun GR (2001) Perceptual load and visuocortical processing:
613 event-related potentials reveal sensory-level selection. *Psychol Sci* 12:213–218.
- 614 Kaynezhad P, Mitra S, Bale G, Bauer C, Lingam I, Meehan C, Avdic-Belltheus A, Martinello
615 KA, Bainbridge A, Robertson NJ, Tachtsidis I (2019) Quantification of the severity of
616 hypoxic-ischemic brain injury in a neonatal preclinical model using measurements of
617 cytochrome-c-oxidase from a miniature broadband-near-infrared spectroscopy system.
618 *Neurophotonics* 6:1.
- 619 Konstantinou N, Bahrami B, Rees G, Lavie N (2012) Visual Short-term Memory Load Reduces
620 Retinotopic Cortex Response to Contrast. *J Cogn Neurosci* 24:2199–2210.
- 621 Konstantinou N, Beal E, King J-R, Lavie N (2014) Working memory load and distraction:
622 dissociable effects of visual maintenance and cognitive control. *Attention, Perception,*
623 *Psychophys* 76:1985–1997.
- 624 Konstantinou N, Lavie N (2013) Dissociable roles of different types of working memory load
625 in visual detection. *J Exp Psychol Hum Percept Perform* 39:919–924.
- 626 Lauritzen M, Mathiesen C, Schaefer K, Thomsen KJ (2012) Neuronal inhibition and
627 excitation, and the dichotomic control of brain hemodynamic and oxygen responses.
628 *Neuroimage* 62:1040–1050.
- 629 Lavie N (2005) Distracted and confused?: selective attention under load. *Trends Cogn Sci*
630 9:75–82.
- 631 Lavie N, Beck DM, Konstantinou N (2014) Blinded by the load: attention, awareness and the
632 role of perceptual load. *Philos Trans R Soc B Biol Sci* 369:20130205.

- 633 Lavie N, Hirst A, de Fockert JW, Viding E (2004) Load theory of selective attention and
634 cognitive control. *J Exp Psychol Gen* 133:339–354.
- 635 Lennie P (2003) The cost of cortical computation. *Curr Biol* 13:493–497.
- 636 Lin A-L, Fox PT, Hardies J, Duong TQ, Gao J-H (2010) Nonlinear coupling between cerebral
637 blood flow, oxygen consumption, and ATP production in human visual cortex. *Proc Natl*
638 *Acad Sci U S A* 107:8446–8451.
- 639 Lindquist MA, Meng Loh J, Atlas LY, Wager TD (2009) Modeling the hemodynamic response
640 function in fMRI: Efficiency, bias and mis-modeling. *Neuroimage* 45:S187–S198.
- 641 Logothetis NK (2008) What we can do and what we cannot do with fMRI. *Nature* 453:869–
642 878.
- 643 Macdonald JSP, Lavie N (2008) Load induced blindness. *J Exp Psychol Hum Percept Perform*
644 34:1078–1091.
- 645 Molloy K, Griffiths TD, Chait M, Lavie N (2015) Inattentional Deafness: Visual Load Leads to
646 Time-Specific Suppression of Auditory Evoked Responses. *J Neurosci* 35:16046–16054.
- 647 Molloy K, Lavie N, Chait M (2019) Auditory figure-ground segregation is impaired by high
648 visual load. *J Neurosci* 39:1699–1708.
- 649 Murphy G, Greene CM (2016) Perceptual Load Induces Inattentional Blindness in Drivers.
650 *Appl Cogn Psychol* 30:479–483.
- 651 Nagamatsu LS, Voss M, Neider MB, Gaspar JG, Handy TC, Kramer AF, Liu-Ambrose TYL
652 (2011) Increased cognitive load leads to impaired mobility decisions in seniors at risk
653 for falls. *Psychol Aging* 26:253–259.

- 654 Navon D, Gopher D (1979) On the economy of the human-processing system. *Psychol Rev*
655 86:214–255.
- 656 Ohta H, Yamada T, Watanabe H, Kanai C, Tanaka E, Ohno T, Takayama Y, Iwanami A, Kato N,
657 Hashimoto R (2012) An fMRI study of reduced perceptual load-dependent modulation
658 of task-irrelevant activity in adults with autism spectrum conditions. *Neuroimage*
659 61:1176–1187.
- 660 Parks NA, Beck DM, Kramer AF (2013) Enhancement and suppression in the visual field
661 under perceptual load. *Front Psychol* 4:275.
- 662 Pasternak T, Greenlee MW (2005) Working memory in primate sensory systems. *Nat Rev*
663 *Neurosci* 6:97–107.
- 664 Peeters-Scholte C, van den Tweel E, Groenendaal F, van Bel F (2004) Redox state of near
665 infrared spectroscopy-measured cytochrome aa3 correlates with delayed cerebral
666 energy failure following perinatal hypoxia-ischaemia in the newborn pig. *Exp Brain Res*
667 156:20–26.
- 668 Phan P, Highton D, Lai J, Smith M, Elwell C, Tachtsidis I (2016) Multi-channel multi-distance
669 broadband near-infrared spectroscopy system to measure the spatial response of
670 cellular oxygen metabolism and tissue oxygenation. *Biomed Opt Express* 7:4424.
- 671 Pinsk MA, Doniger GM, Kastner S (2004) Push-pull mechanism of selective attention in
672 human extrastriate cortex. *J Neurophysiol* 92:622–629.
- 673 Raichle ME, Gusnard DA (2002) Appraising the brain's energy budget. *Proc Natl Acad Sci*
674 99:10237–10239.

- 675 Raichle ME, MacLeod AM, Snyder AZ, Powers WJ, Gusnard DA, Shulman GL (2001) A default
676 mode of brain function. *Proc Natl Acad Sci* 98:676–682.
- 677 Rees G (1999) Inattentional Blindness Versus Inattentional Amnesia for Fixated But Ignored
678 Words. *Science* (80-) 286:2504–2507.
- 679 Rees G, Frith CD, Lavie N (1997) Modulating irrelevant motion perception by varying
680 attentional load in an unrelated task. *Science* 278:1616–1619.
- 681 Schwartz S, Vuilleumier P, Hutton C, Maravita A, Dolan RJ, Driver J (2005) Attentional load
682 and sensory competition in human vision: modulation of fMRI responses by load at
683 fixation during task-irrelevant stimulation in the peripheral visual field. *Cereb cortex*
684 15:770–786.
- 685 Schwartz WJ, Smith CB, Davidsen L, Savaki H, Sokoloff L, Mata M, Fink DJ, Gainer H (1979)
686 Metabolic mapping of functional activity in the hypothalamo- neurohypophysial system
687 of the rat. *Science* (80-).
- 688 Siddiqui MF, Lloyd-Fox S, Kaynezhad P, Tachtsidis I, Johnson MH, Elwell CE (2018) Changes in
689 Cytochrome-C-Oxidase Account for Changes in Attenuation of Near-Infrared Light in
690 the Healthy Infant Brain. In: *Advances in Experimental Medicine and Biology*, pp 7–12.
- 691 Silvanto J, Muggleton N, Lavie N, Walsh V (2009) The Perceptual and Functional
692 Consequences of Parietal Top-Down Modulation on the Visual Cortex. *Cereb Cortex*
693 19:327–330.
- 694 Simons DJ, Chabris CF (1999) Gorillas in our midst: sustained inattention blindness for
695 dynamic events. *Perception* 28:1059–1074.

- 696 Sokoloff L, Mangold R, Wechsler RL, Kennedy C, Kety SS (1955) The effect of mental
697 arithmetic on cerebral circulation and metabolism. *J Clin Invest* 34:1101–1108.
- 698 Stolte M, Bahrami B, Lavie N (2014) High perceptual load leads to both reduced gain and
699 broader orientation tuning. *J Vis* 14:9–9.
- 700 Tisdall MM, Tachtsidis I, Leung TS, Elwell CE, Smith M (2008) Increase in cerebral aerobic
701 metabolism by normobaric hyperoxia after traumatic brain injury. *J Neurosurg*
702 109:424–432.
- 703 Torralbo A, Kelley TA, Rees G, Lavie N (2016) Attention induced neural response trade-off in
704 retinotopic cortex under load. *Sci Rep* 6:33041.
- 705 Wei P, Szameitat AJ, Müller HJ, Schubert T, Zhou X (2013) The neural correlates of
706 perceptual load induced attentional selection: An fMRI study. *Neuroscience* 250:372–
707 380.
- 708 Whiteley L, Sahani M (2012) Attention in a Bayesian Framework. *Front Hum Neurosci* 6:100.
- 709 Wickens CD, Vidulich M, Sandry-Garza D (1984) Principles of S-C-R Compatibility with Spatial
710 and Verbal Tasks: The Role of Display-Control Location and Voice-Interactive Display-
711 Control Interfacing. *Hum Factors J Hum Factors Ergon Soc* 26:533–543.
- 712 Wojciulik E, Kanwisher N (1999) The Generality of Parietal Involvement in Visual Attention.
713 *Neuron* 23:747–764.
- 714 Ye JC, Tak S, Jang KE, Jung J, Jang J (2009) NIRS-SPM: Statistical parametric mapping for
715 near-infrared spectroscopy. *Neuroimage* 44:428–447.
- 716 Yi D-J, Woodman GF, Widders D, Marois R, Chun MM (2004) Neural fate of ignored stimuli:

717 dissociable effects of perceptual and working memory load. Nat Neurosci 7:992–996.

718

719

720

721

722

723

724

725

726

727

728

729

730

731

732

733

734

735 **Tables**

736 **Table 1: Average Channel Positions and Brodmann Area Allocations in Experiment 1**

Channel	MNI Coordinate			Brodmann Areas	Probability
	X	Y	Z		
1	-54.73	-76.19	12.31		
				19	0.63
				37	0.21
				39	0.15
2	-43.38	-89.02	16.77		
				18	0.12
				19	0.88
3	-51.31	-80.27	-6.40		
				19	0.90
				37	0.10

4	-42.29	-92.29	-2.92		
				18	0.56
				19	0.44
5	-28.88	-97.85	18.40		
				17	0.28
				18	0.51
				19	0.21
6	-12.98	- 103.90	19.06		
				17	0.83
				18	0.17
7	-28.25	- 102.60	-0.15		
				17	0.62
				18	0.38

8	-13.98	- 107.77	1.63		
				17	1.00
9	7.17	- 100.92	17.15		
				17	0.74
				18	0.26
10	24.00	- 101.54	15.94		
				17	0.76
				18	0.24
11	6.40	- 102.69	1.50		
				17	1.00

12	22.79	- 104.94	-1.96		
				17	0.86
				18	0.14
13	39.23	-92.13	13.04		
				17	0.05
				18	0.49
				19	0.46
14	52.94	-79.10	9.52		
				19	0.79
				37	0.15
				39	0.06
15	37.50	-95.50	-6.00		

				18	0.93
				19	0.07
16	48.52	-83.44	-10.63		
				18	0.03
				19	0.97

737 **Table 1.** Overview of group-averaged MNI coordinates and assignment to Brodmann Areas in Experiment 1.

738 **Table 2: Average Channel Positions and Brodmann Area Allocations in Experiment 2**

Channel	MNI Coordinates			Brodmann Area	Probability
	X	Y	Z		
1	-56.94	-70.48	22.33		
				19	0.10
				37	0.08
				39	0.82
2	-45.39	-84.09	25.93		
				19	0.74

				39	0.26
3	-54.56	-76.91	0.13		
				19	0.66
				37	0.34
4	-44.83	-89.89	3.28		
				18	0.39
				19	0.61
5	-30.20	-93.74	26.07		
				18	0.50
				19	0.50
6	-14.20	-99.93	25.78		
				17	0.35
				18	0.65

7	-30.57	- 100.80	3.91		
				17	0.50
				18	0.50
8	-14.76	- 107.39	4.43		
				17	1.00
9	7.52	-97.67	24.81		
				17	0.21
				18	0.75
				19	0.03
10	24.81	-95.87	26.31		
				17	0.08
				18	0.89

				19	0.03
11	7.00	- 103.59	4.57		
				17	1.00
12	24.67	- 103.98	4.98		
				17	0.93
				18	0.07
13	40.96	-86.83	25.76		
				18	0.01
				19	0.95
				39	0.04
14	53.89	-74.43	23.89		
				19	0.13

				37	0.02
				39	0.85
15	39.94	-93.46	3.63		
				17	0.03
				18	0.79
				19	0.18
16	52.24	-80.74	1.83		
				19	0.92
				37	0.08

739 **Table 2.** Overview of group-averaged MNI coordinates and assignment to Brodmann Areas in Experiment 2.

740 **Table 3:** Behavioural Results from Experiment 1

	Low Load	High Load
Reaction Time	491 ms (48)	619 ms (40)
Hit Rate	99.02% (1.76)	95.90% (4.27)
False Alarm Rate	0.03% (0.48)	4.95% (5.00)

741 **Table 3.** Task performance means (SD in brackets) in Experiment 1.

742 **Table 4:** Behavioural Results from Experiment 2

	Low Load	High Load
Reaction Time	510 ms (56)	599 ms (67)
Hit Rate	98.79% (1.61)	95.92% (4.48)
False Alarm Rate	1.16% (1.07)	6.17% (10.11)

743 **Table 4.** Task performance means (SD in brackets) in Experiment 2.

744

745

746

747

748

749

750

751

752

753

754

755

756 **Figure Captions**

757 **Figure 1.** Experimental Design. A: Experimental task in Experiment 1: Participants saw a
758 stream of coloured crosses and had to respond to feature targets in low load (any red cross)
759 or conjunction targets in high load (upright purple or inverted blue crosses). A flickering,
760 radial checkerboard was present on half of the RSVP streams. B: Experimental task in
761 Experiment 2: The size of the crosses was increased and a white pattern was added to
762 increase the strength of the response in visual cortex. Images are not to scale.

763 **Figure 2.** oxCCO concentration changes in Experiment 1. A: Mean (\pm SEM) oxCCO signal per
764 condition (high/low load x checkerboard present/absent) across the task period (25 s) for all
765 investigated regions. B: Difference scores (distractor present minus absent conditions) of
766 the mean oxCCO signals (\pm SEM) by load, illustrating the nature of interactions in Panel A. C:
767 Time series of the group averaged oxCCO signal related to the presence (minus absence) of
768 the unattended stimulus. Grey, shaded areas represent the task period (25 s, followed by a
769 25 s rest period), coloured areas along the graphs represent the SEM. Asterisks indicate
770 statistical significance ($p < .05$). Int = Interaction.

771 **Figure 3.** oxCCO concentration changes in Experiment 2. A: Mean (\pm SEM) oxCCO signal per
772 condition (high/low load x checkerboard present/absent) during the task period (25 s)
773 across all investigated regions. B: Difference score of the mean oxCCO signals (\pm SEM) in the
774 distractor present minus absent conditions plotted as a function of load, illustrating the
775 nature of interactions in Panel A. C, D: Time series of the group averaged oxCCO signal
776 related to the attended (C, distractor absent conditions only) and unattended (D, difference
777 score of present minus absent trials) stimuli. Grey, shaded areas represent the task period

778 (25 s, followed by a 25 s rest period), coloured areas along the graphs represent the SEM.

779 Asterisks indicate statistical significance ($p < .05$). Int = Interaction.

780 **Figure 4.** Time course of the load effects on oxCCO signal associated with attended and
781 unattended stimulus processing. A: Time series of the load effects (high – low) on the oxCCO
782 signal underlying attended and unattended processing are shown for each iteration of the
783 data splitting procedure. Bold lines with matching linetypes indicate 3 specific iteration
784 instances of time series pairs for which the r value was closest to the mean r value across all
785 conditions, shown for illustrative purposes. B: Cumulative mean r values across 1000
786 iterations of the random sample splitting procedure which represents the correlation
787 between the load effects on attended and unattended processing. Grey, shaded error bars
788 represent 95% confidence intervals. The mean r value can be seen to stabilise on the
789 resultant mean after ~200 iterations in all areas. Moreover, the narrow 95% confidence
790 intervals (already found at ~500 iterations) indicate that the resultant mean is a reliable
791 representation of the correlation between the two time series.

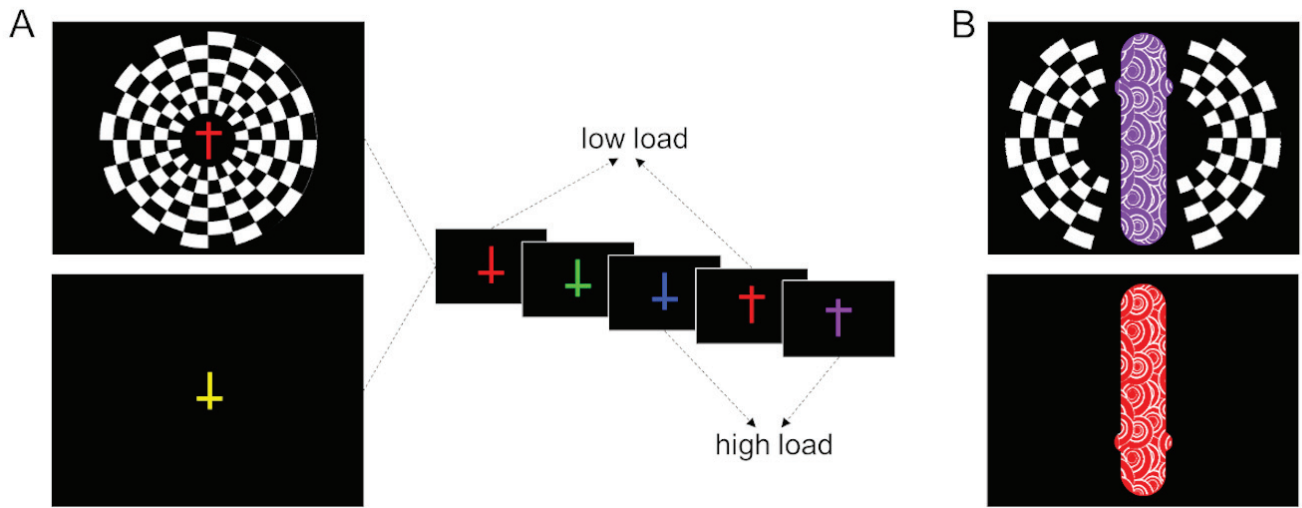
792

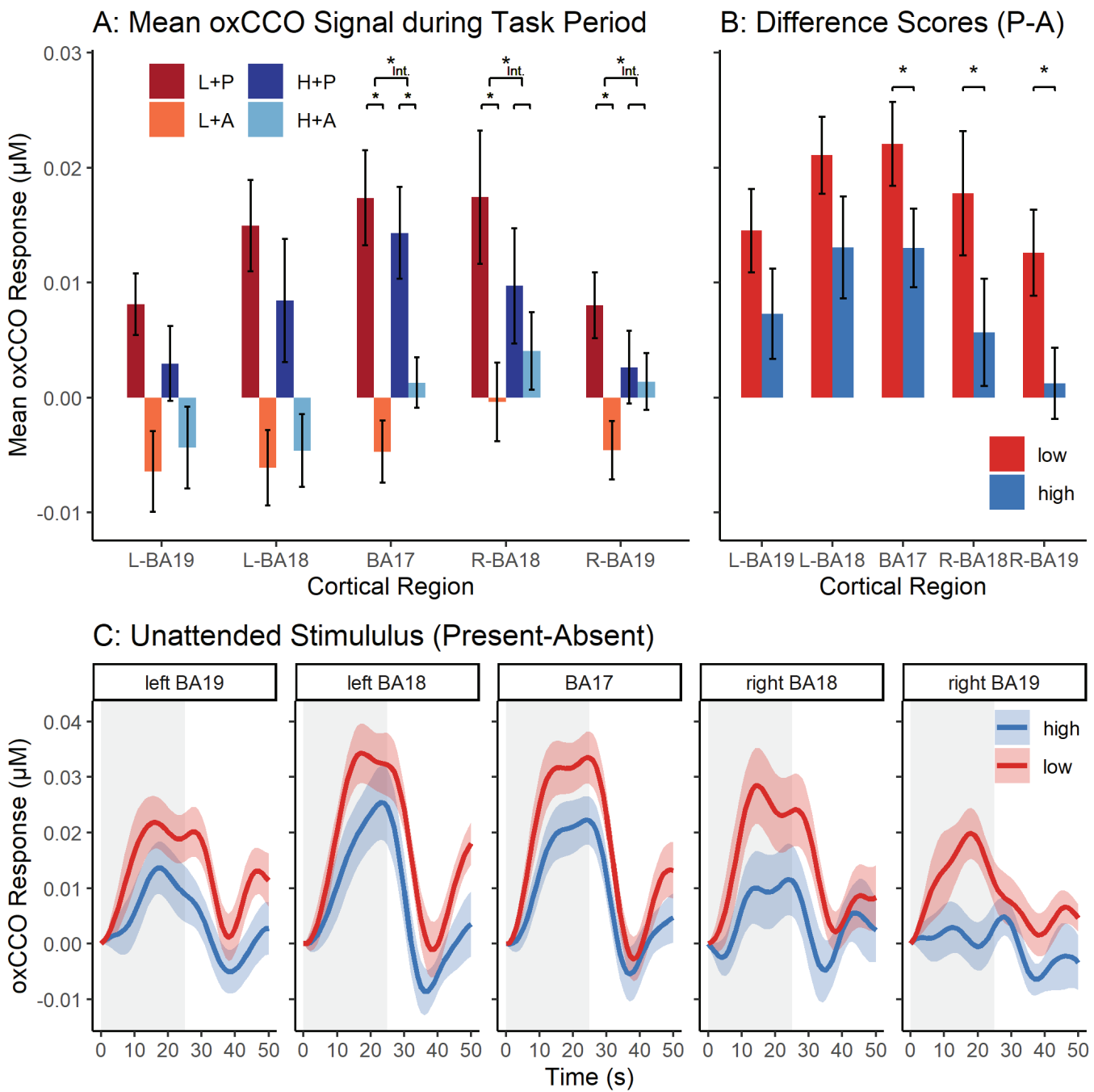
793

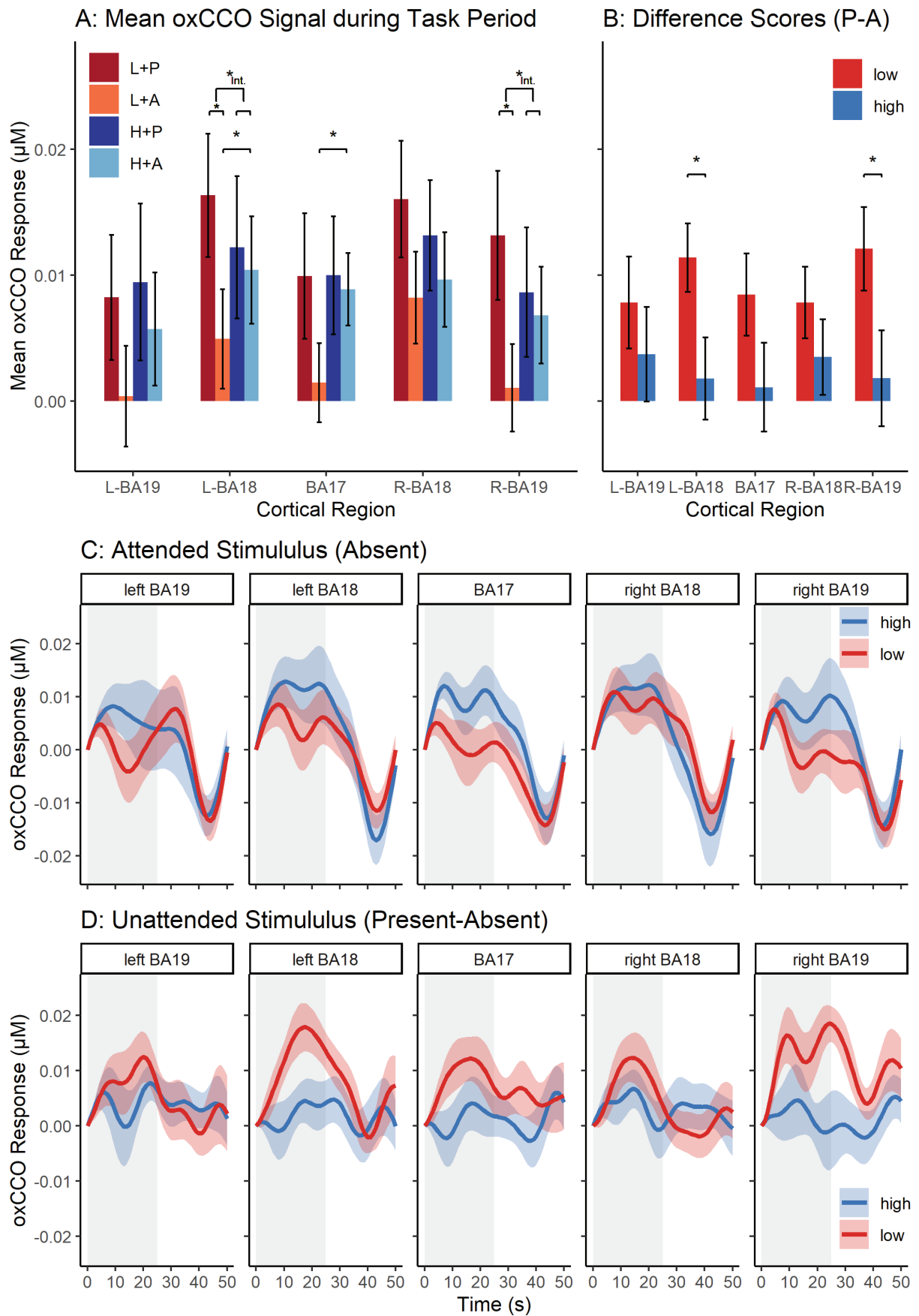
794

795

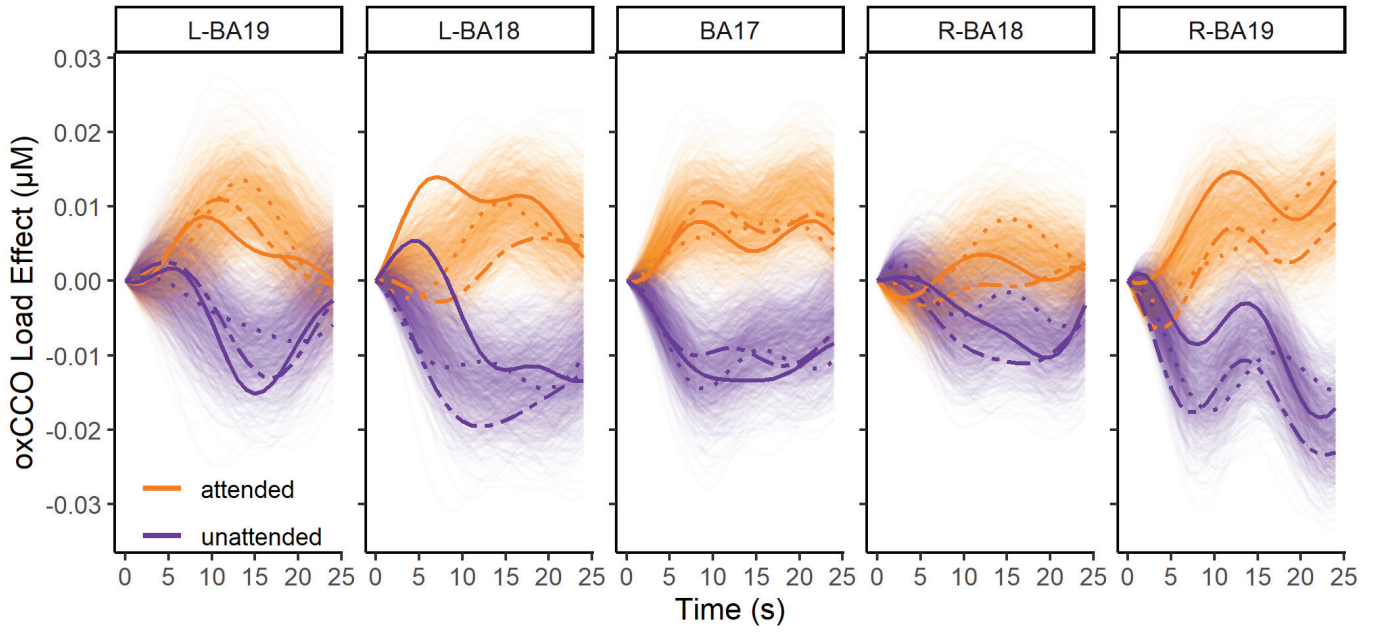
796







A: oxCCO Time Series of Load Effects for Attended and Unattended Stimuli



B: Cumulative Mean r

